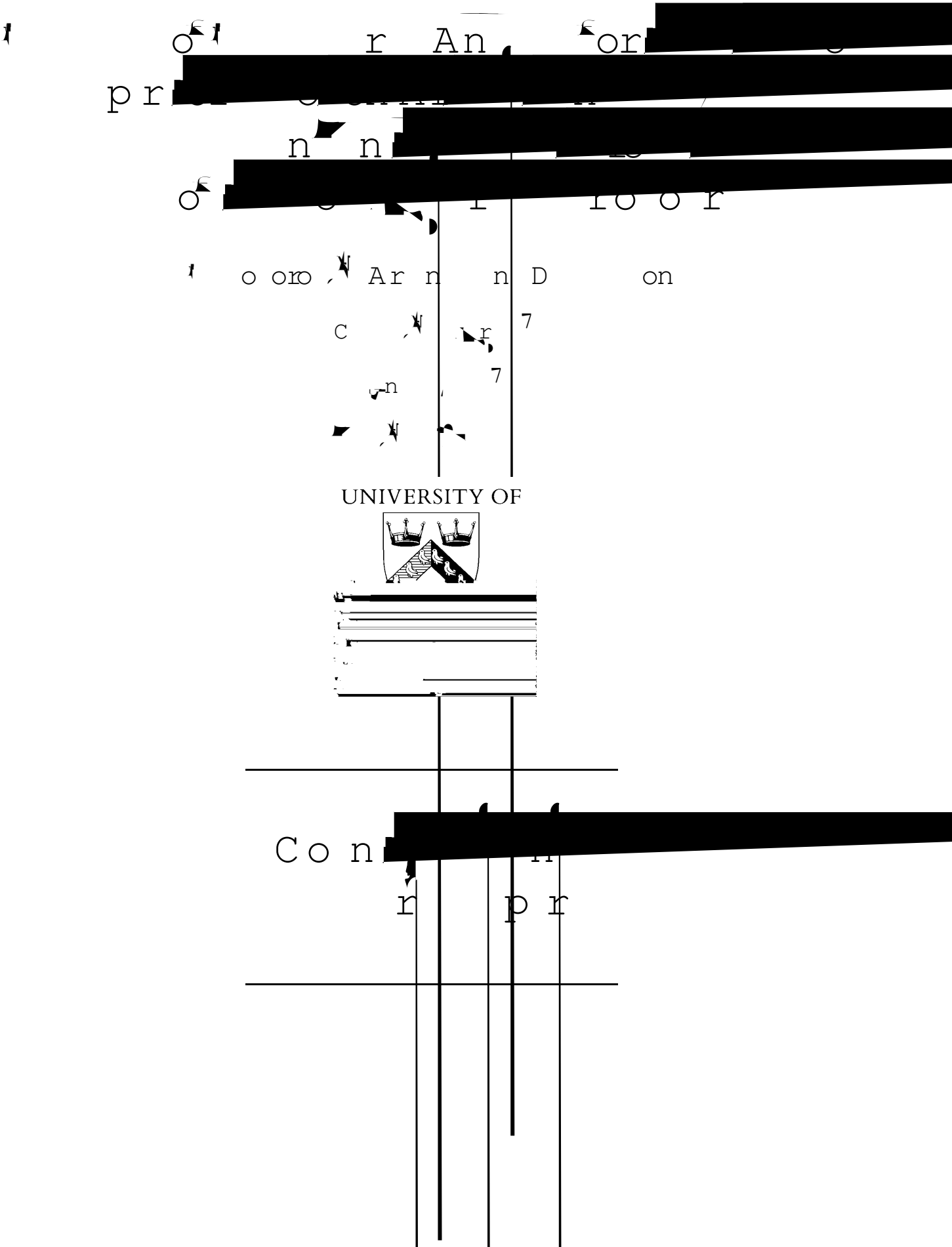

The Use of Time Series Analysis for the

for the understanding of the basic MR physical processes and the analysis of interesting research problems [31, 58].

In general, we can identify two main groups of time series analysis techniques: (a) The *time domain* and (b) the *frequency domain* analysis techniques. The time domain techniques have been investigated extensively by several researchers and characterized as favourable towards the analysis of random processes [16, 26, 45, 46, 47]. On the other hand, frequency domain techniques have been found mostly suitable for the investigation of the opposite to the random processes, the so-called deterministic processes. Additionally, frequency domain analysis has always proven to have advantages for periodic phenomena [12, 15, 36].

In this paper, we examine the issues relating to the problem of respiratory motion artefacts in biomedical magnetic resonance imaging and spectroscopy, through the use of time series analysis on MR artefacted data. In particular, we introduce the use of the **Lomb-Scargle periodogram** for the analysis of k-space data, and investigate its appearance and properties when applied to MR images and spectra that have been "contaminated" by motion artefacts. In the first part of this paper, we provide the reader with the appropriate theoretical background and discuss our motivation for using this frequency domain technique as as

in many scientific fields, mainly towards the solution of the signal detection problem [27, 29, 32, 45, 55].

The signal detection problem, as described in various signal and image processing textbooks [24, 45, 51, 55], can be formulated as follows. Suppose that a physical variable H is measured at a set of times t_i[2]. This measurement results in a time-series data, here denoted as $\{H(t_i), i = 1, 2, 3, ..., N\}$, which is called the observed digitized signal. This data set is assumed to be the sum of a pure signal and random observational errors. Consequently, the times series data can be represented by the following expression [24]:

$$H_i = H(t_i) = S(t_i) + N(t_i) \tag{1}$$

where $S(t_i)$ is the pure signal and $N(t_i)$ represents the observational errors during the measurement of the signal. Because of the additive relationship between the pure (or original) signal and the parameter $N(t_i)$ in equation (1), the latter is often called the **noise**. For many applications of the signal detection theory, the noise is assumed to be random [24, 38, 40, 56], which means that the observational errors at distinct times are statistically independent. Furthermore, in a significant number of cases, the noise is usually assumed to have a normal distribution with zero mean and constant variance σ_o^2, hence the term "Gaussian noise" [24, 40].

In many scientific measurement applications, noise can badly corrupt the observed signal. The main motivation behind the signal detection theory is the solution to this problem, that is to establish the existence of a signal in the presence of noise. In addition to this, researchers used the framework provided by the theory to investigate other important problems. For example, one might want to identify the presence of a periodicity in a "noisy" signal or estimate the harmonic content of a periodic signal (either by the detecting the principal signal harmonic or its multiple). Other interesting problems are the frequency or period calculation of a particular signal harmonic and the removal of random noise from the observed signal. In the context of the Lomb-Scargle formulation,

$$S_i' = S(t_i)' = S(t_i) + G(t_i) + N(t_i) \tag{2}$$

can be evaluated at any frequency, it is traditionally evaluated only at a special set of $N' = N/2$ evenly spaced frequencies [21, 23, 43, 52]. However, this particular definition of the classical periodogram has two important problems:

1. The classical periodogram presents several statistical difficulties. This, in simple words, means that the function $P(\omega)$ of the periodogram is very noisy [52, 57] and several techniques for further processing and optimization are required.

2. There exists the major problem of spectral leakage [20, 44, 51]. This means that for any periodic signal at a specific frequency, the power in the periodogram does not appear only at that frequency, but also "leaks" into other frequencies (a typical example of spectral leakage is the well-known phenomenon of aliasing [14, 17, 18]). In the literature there exists a significant amount of work describing the problem of spectral leakage and the related techniques used to overcome the "leakage" effects. [10, 33, 59].

Furthermore, this definition does not cope with data sets that are not evenly sampled. For this reason, Scargle [54] derived a new definition of the periodogram, which will be described in the following section. Because of some interesting similarities to a power spectrum estimation technique that Lomb formulated on 1976, we will call this periodogram the Lomb-Scargle periodogram.

2.3 The Lomb Scargle Periodogram

As already mentioned in the previous section, the classical periodogram and its statistical distribution have been successfully investigated for the case of evenly sampled data sets. Usually, the distribution of the power spectrum has an exponential shape. This has been shown for the case in which the evenly sampled data set $g(t_i)$ is pure Gaussian noise [30]. A similar result has been derived for the more general case of data sets with uneven sampling. Thus, a modified version of the classical periodogram has been defined by Jeffrey Scargle – an eminent researcher at the NASA Ames Research Center – to cope with the case of unevenly sampled data sets [54]. The power spectrum estimate provided by the modified periodogram has the same exponential distribution as in the even-sampling case [11, 34, 49, 50, 54]:

$$P(\omega) = \frac{1}{2}\left\{ \frac{\left[\sum_{i=0}^{N-1} g(t_i)\cos\omega(t_i-\tau)\right]^2}{\sum_{i=0}^{N-1}\cos^2\omega(t_i-\tau)} + \frac{\left[\sum_{i=0}^{N-1} g(t_i)\sin\omega(t_i-\tau)\right]^2}{\sum_{i=0}^{N-1}\sin^2\omega(t_i-\tau)} \right\} \quad (6)$$

where $i = 0, 1, 2, ..., N-1$ is the index of the unevenly spaced observation times. The term τ can be defined by the following expression:

$$\tan 2\omega\tau = \frac{\left(\sum_{i=0}^{N-1}\sin\omega t_i \right.}{} \quad \textit{of}$$

t t *t ititio of t djt*

Scargle argues

null hypothesis, the power spectrum $P(\omega)$ (and in effect the power at a given frequency) has an exponential distribution with zero mean and noise variance

2.5 The False Alarm Probability

It is desired to find a power level, z_o, such that if the power exceeds this level, the error in declaring a detected peak as being significant will be very small. The probability of this fault, p_o, is called the false alarm probability of the null hypothesis and it can be fixed to be a small number, so that the detected peaks have high significance. The above mentioned threshold power level can be derived by the distribution in equation (12) and is given by the following expression:

$$z_o = -\ln[1-(1-p_o)^{1/M}] \tag{14}$$

where M are the independent observed frequencies used in the calculation of the normalized Lomb-Scargle periodogram.

For small p_o, equation (14) becomes

$$z_o \approx \ln(M/p_o) \tag{15}$$

For example, if we take $p_o = 0.01$, which means we have a 99% significance level, then z_o is given by the following expression:

$$z_o \approx 4.6 + \ln(M) \tag{16}$$

We will use expressions (15) and (16) to identify the significance levels of the experimental results presented in the second part of this chapter.

3 Time-Series Analysis and Respiratory Motion Artefacts in MR: The Reasoning Behind the Use of the Lomb-Scargle Periodogram

As we have argued in a previously published study [6], the effect of motion in spectroscopic Chemical Shift Imaging (CSI) is manifested in the appearance of spectra as signal re-distribution and as an overall increase in the background noise level. Our initial experience in both cardiac and hepatic ^{31}P MRS studies on volunteers showed small (5–10%) but consistent improvements in the overall signal-to-noise ratio (SNR) of the spectra when the Respiratory Ordered Phase Encoding (ROPE) method was used. On the spectra, these changes appeared to be visually more significant in the level and the character of the noise, rather than in the signal level itself. These visual observations have suggested the importance of further understanding the source and appearance of motion artefacts in spectroscopic CSI investigations. Thus, we used the autocorrelation function, a typical Fourier transform time-series analysis approach, to identify the character of random and systematic noise (motion artefacts) upon both 2D-FT imaging and 1D CSI spectroscopic data. The selection of this technique was based on the opinion that the autocorrelation function of time series data completely specifies the first- and second-order noise statistics of Gaussian processes [24]. We applied both the one-dimensional and the two-dimensional versions of the autocorrelation function in data from phantom MRI and MRS studies. The result of this time series analysis investigation showed high order correlations arising from motion artefact effects. Furthermore, when comparing

the three cases of image acquisitions of a moving phantom, a static phantom and a moving ROPE'd phantom, we identified significant differences in their MR data autocorrelation functions.

Although these results were found promising at the time, all observations were purely qualitative. There was still a need to quantify these results, so that we could have precise information about the correlation of motion with any time series analysis of the MR data. In order to satisfy this need we investigated time series analysis techniques even further. The technique we adopted was the power spectrum estimation of the MR data by means of periodogram analysis.

In the past, Weisskoff et al. had applied the classical Fourier periodogram

bined for each data point. As

diameter) – was used for the creation of k-space data. We created image data corresponding to image acquisitions for both stationary and moving objects. Furthermore, we also acquired simulated data corresponding to images corrected by the ROPE method. All k-space matrices that we constructed were of size 64×64. We reduced the 2D matrices to single 1D arrays of 4096 data points, thus treating the FID signals in the data as a single time series signal, unevenly sampled. These data points together with the corresponding observation times[6] constituted the input data for the normalized Lomb-Scargle periodogram. In this case we evaluated the periodogram at 8,192 independent frequencies. No prior processing of the data was performed, and the periodogram was evaluated for the magnitude of the FID signals.

As well as using simulated data, we performed periodogram analysis on actual experimental MRI and MRS data sets. All experimental work was carried out on a Picker prototype MRI/MRS system, operating at a field of 1.5 Tesla, at the Robert Steiner MRI Unit, Hammersmith Hospital, London.

The subject of the study was a simple phantom [7, 22], constructed with non-magnetic materials (Perspex and plastic). This phantom consisted of a cylinder (height 10 cm, diameter 5 cm), filled with a $CuSO_4$ solution. A mechanical device was designed to provide a variable vertical displacement of the cylinder. The phantom was mechanically coupled by the use of a long shaft to a DC step electric motor positioned 6 meters away from the centre of the bore of the main magnet. The electric motor provided the driving mechanism that applied periodic displacement on the phantom. The amplitude and the period of the displacement could be varied in order to model the effects of human respiratory motion. Figures 1 and 2 show the profile and semi-lateral photographic views of the phantom.

We acquired data by using both 2D-FT imaging and 1D spectroscopic CSI methods. Images and spectra were obtained for the

Figure 1: Profile view of the experimental phantom

In the following section we observe representative results from our simulated and experimental work.

5 Results

5.1 Periodogram Analysis on Simulated Image Data

We collected a set of representative periodogram results of 2D-FT imaging data, originating from a simulated point-like object. In this set of experiments, the object was moving with a motion amplitude set at 15 pixels. For each row of the data matrices, data points were sampled every 0.04 msec of simulated time at 500 msec TR intervals. These imaging parameters were kept constant for all experiments. The only factor that was altered was the period of the movement of the object. For four different frequencies of motion, we compared the appearance of the periodogram using data from the moving object and data that was controlled by our implementation of the Respiratory Ordered Phase Encoding (ROPE) method. These periodograms were further compared to the appearance of the Lomb-Scargle periodogram of image data of a static object.

As mentioned in the previous section, the periodogram was evaluated at 8,192 independent frequencies, ranging from 0 kHz to the periodogram's experimental Nyquist frequency, which for this case was 64 kHz[7]. For convenience, we compared all results by studying the periodogram in a window around the maximum observed peak.

[7] The total simulated time of the imaging experiment was 32 sec. One can calculate the periodogram's experimental Nyquist frequency by dividing the total number of points in the data set by twice the total imaging time.

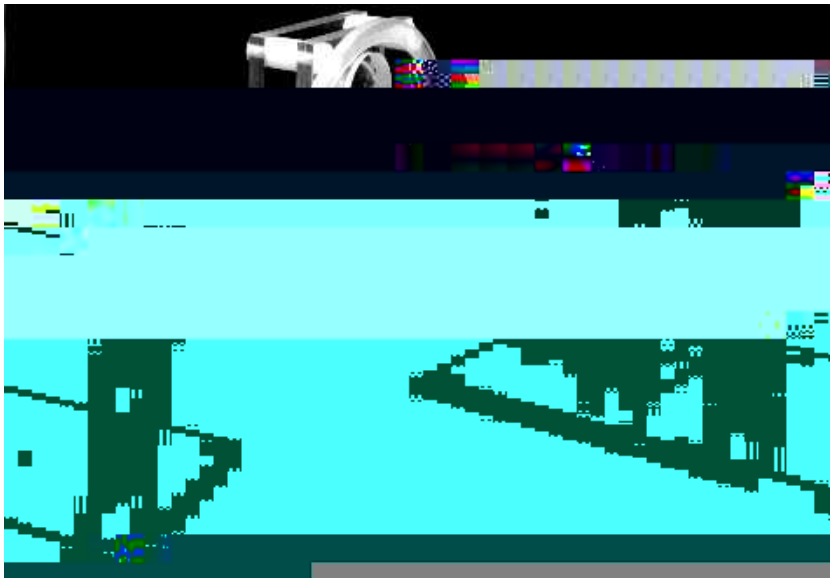

Figure 2: Semi-lateral view of the experimental phantom

The significance of the power spectrum levels has been evaluated by using the false alarm probability condition, as given by equation (14).

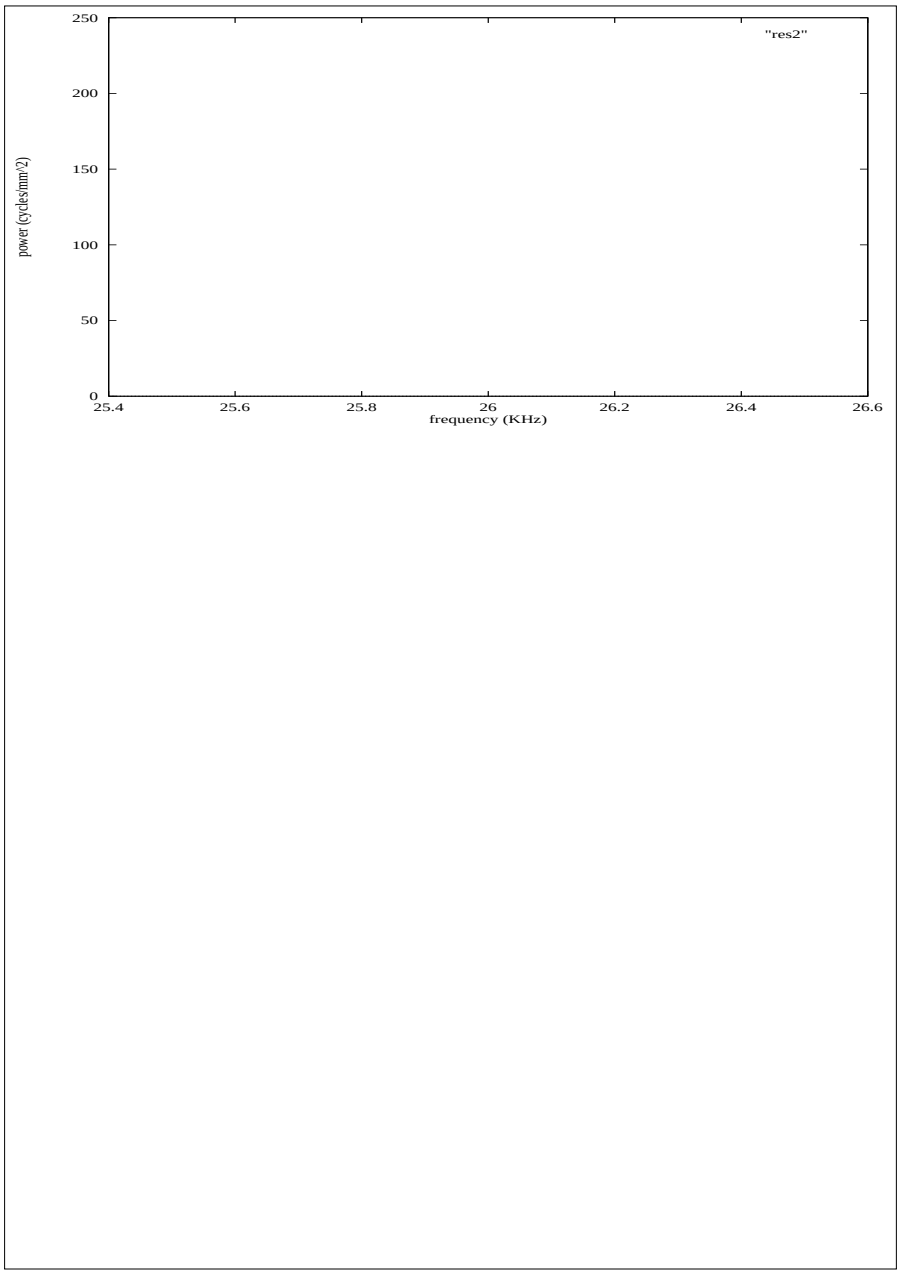
"res2"
250
200
150
100
50
0
power (cycles/mm^2)
25.4
25.6
25.8
26
26.2
26.4
26.6
frequency (KHz)

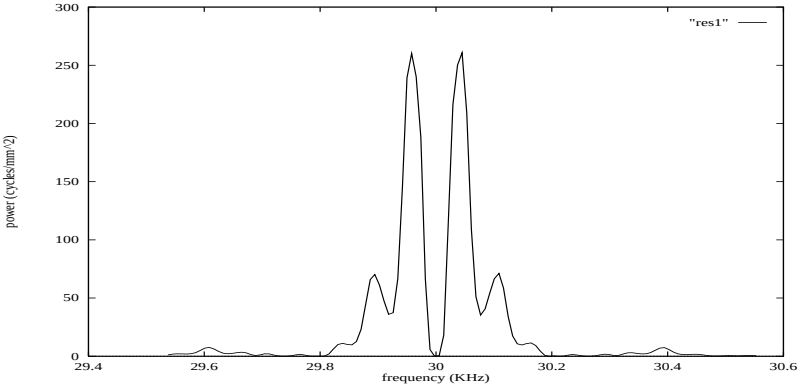
"res1"
power (cycles/mm^2)
frequency (KHz)
300
250
200
150
100
50
0
29.4
29.6
29.8
30
30.2
30.4
30.6


40
20
0

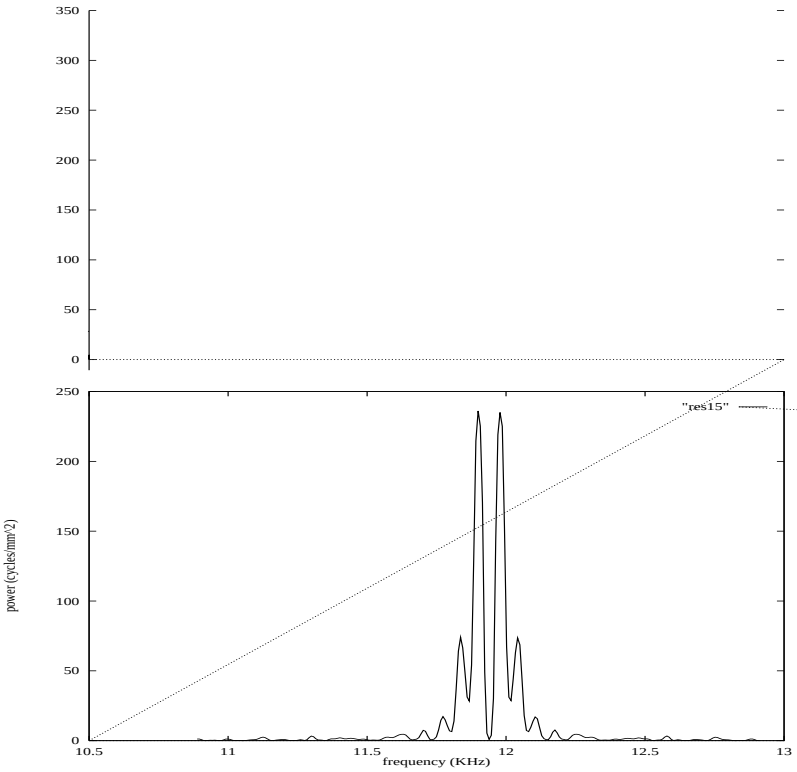
350
300
250
200
150
100
50
0
250
200
150
100
50
0
"res15"
power (cycles/mm^2)
10.5
11
11.5
12
12.5
13
frequency (KHz)

cycles/mm^2)

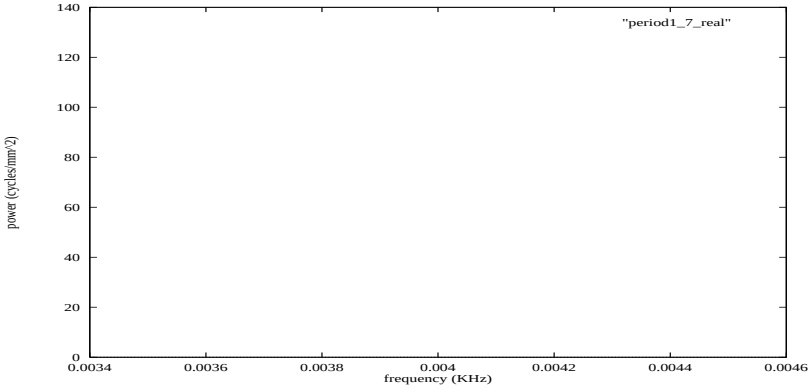
"period1_7_real"
power (cycles/mm^2)
frequency (KHz)
140
120
100
80
60
40
20
0
0.0034
0.0036
0.0038
0.004
0.0042
0.0044
0.0046

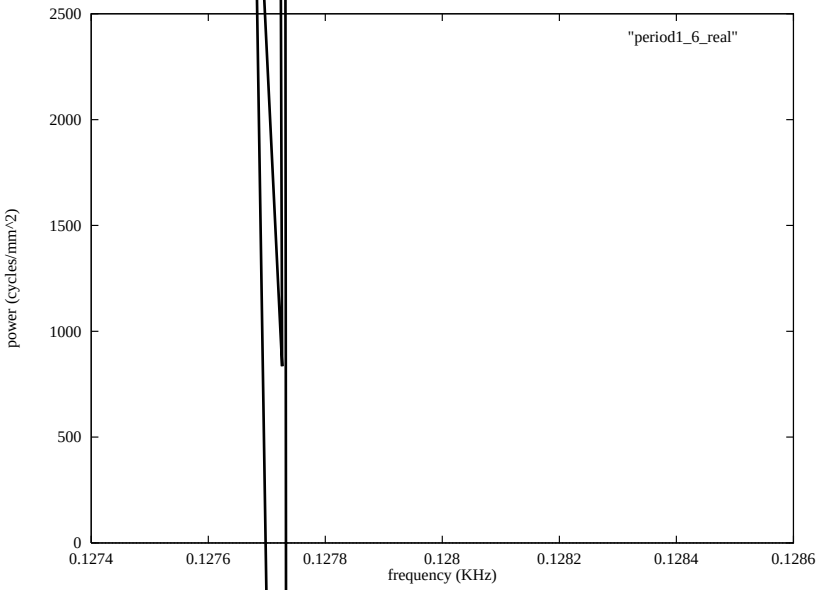
"period1_6_real"
2500
2000
1500
1000
500
0
power (cycles/mm^2)
0.1274
0.1276
0.1278
0.128
0.1282
0.1284
0.1286
frequency (KHz)

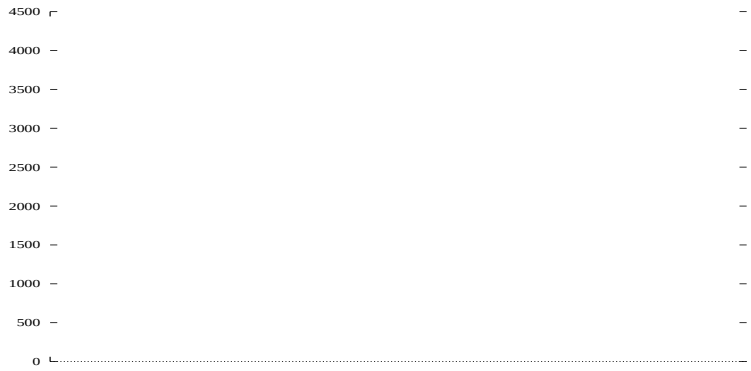
4500
4000
3500
3000
2500
2000
1500
1000
500
0

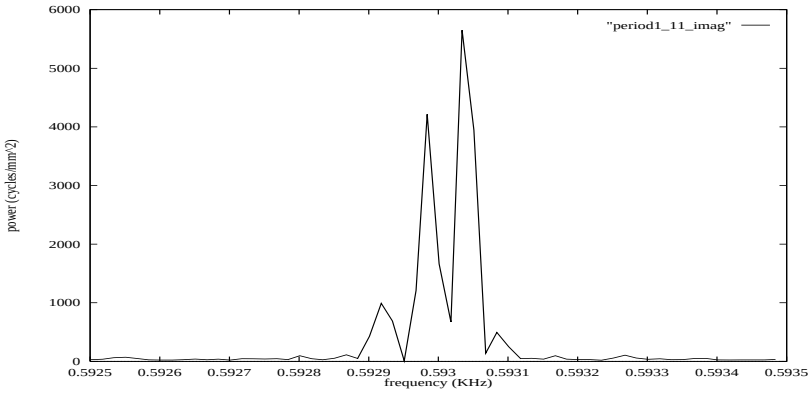
"period1_11_imag"
power (cycles/mm^2)
frequency (KHz)
6000
5000
4000
3000
2000
1000
0
0.5925
0.5926
0.5927
0.5928
0.5929
0.593
0.5931
0.5932
0.5933
0.5934
0.5935

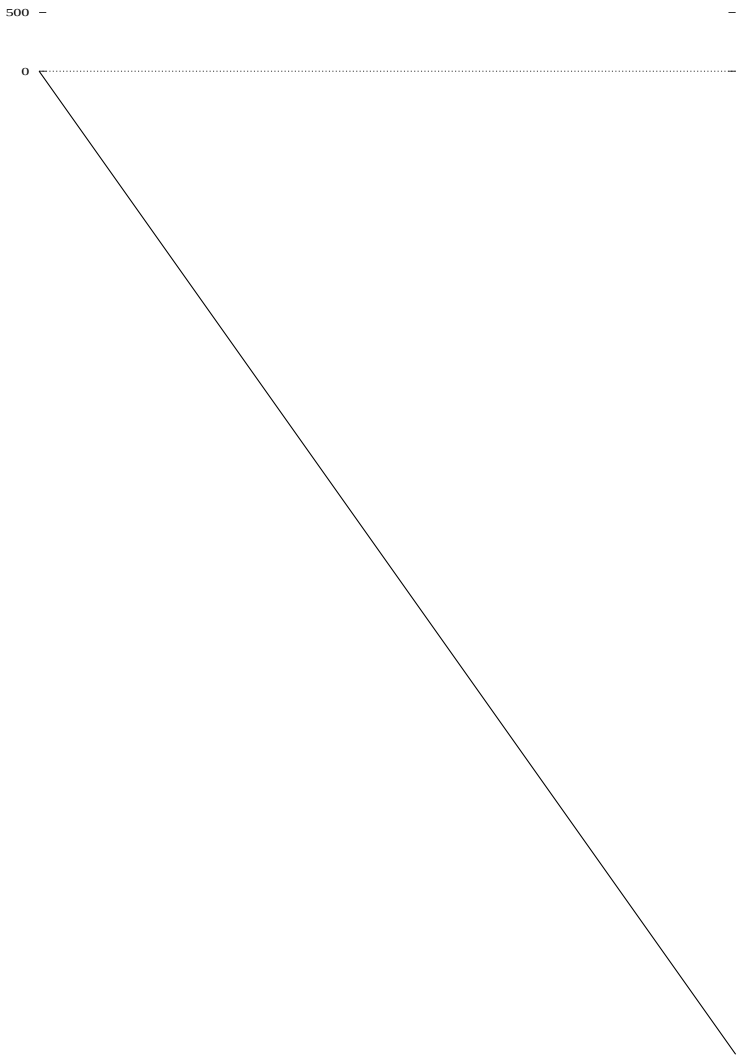
500
0

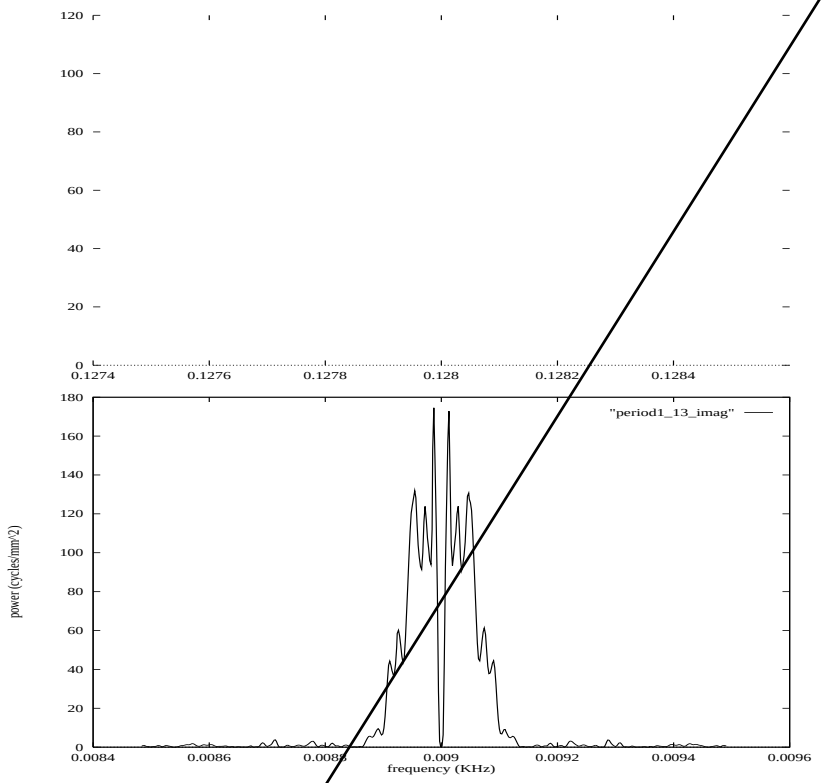
120
100
80
60
40
20
0
0.1274
0.1276
0.1278
0.128
0.1282
0.1284
180
160
140
120
100
80
60
40
20
0
0.0084
0.0086
0.0088
0.009
0.0092
0.0094
0.0096
"period1_13_imag"
power (cycles/mm^2)
frequency (KHz)

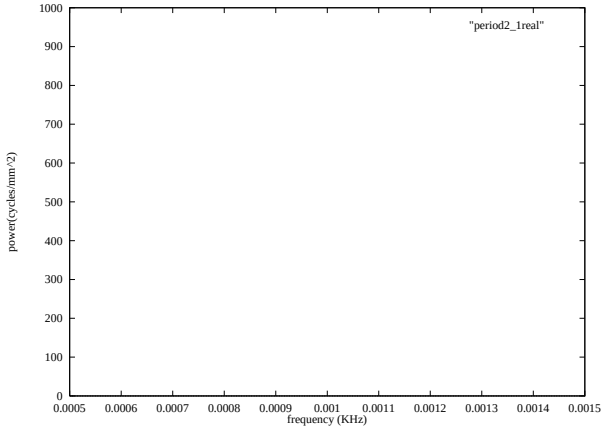
"period2_1real"
power(cycles/mm^2)
frequency (KHz)
1000
900
800
700
600
500
400
300
200
100
0
0.0005
0.0006
0.0007
0.0008
0.0009
0.001
0.0011
0.0012
0.0013
0.0014
0.0015

to "put back" the artefact on the original signal. However, as seen in both real (8.A) and imaginary (8.B) parts of the data set, lower harmonics exist within the area of the main signal, although a successful ROPE correction has been accomplished. This again may correspond to the inability of ROPE to correct high-order ghosts and to deal with the effects of blurring.

The other observations made on the examples of data with different matrix size and averaged artefacted data are purely qualitative and prove once again some known factors that increase or reduce the intensity of the motion artefact. This result enhances our position that the Lomb-Scargle periodogram cannot be used as a quantitative tool for assessing k-space MR data. Moreover, this fact forbids the technique from being used as an indicator for the control of the motion artefact. However, the results found in the case of MR spectroscopic data are more promising. The visual observation of the periodogram of both the artefacted and ROPE'd spectroscopic data proves that the observed noise levels on spectra might originate from systematic errors as well. Our study showed that the motion artefact in MRS may be characterized by three factors in the Lomb-Scargle periodogram:

- The existence of significant harmonics, additional to the power of the signal.
- The reduced total power, observed on the maximum peak $P(f_{\max})$
- The increased level of random noise.

The above indicators, although at this stage qualitative, suggest that the Lomb-Scargle method could be more generally used as a diagnostic tool for identifying other systematic errors in human *in vivo* spectroscopic experiments.

7 Conclusion

Our study strongly suggests that the Lomb-Scargle periodogram can offer interesting qualitative information, relating to the effect of motion artefacts in both clinical MRS and MRI. Our observations, in particular for the case of MRS, lead us to the conclusion that the Lomb-Scargle periodogram could be more generally used as a diagnostic tool for identifying technical errors in human *in vivo* spectroscopic experiments. At present, the fast algorithm calculates the periodogram within a time span of four minutes, even for large data sets consisting of 65,536 points. Appropriate code optimization can improve the calculation time of the periodogram. Then, this technique can be used in real-time as a quick diagnostic method of the state of spectroscopic systems. If necessary, the MRS system can then be re-calibrated or an appropriate action to eliminate systematic errors can be taken.

We believe that through this paper we offer a new point of view in the study of the respiratory motion artefacts in MRI and MRS. Moreover, we have identified a new technical diagnostic tool that can be further developed and used to detect systematic errors in MR systems.

Acknowledgments

The authors would like to acknowledge Prof. Ian Young and Dr David Bryant for providing the collaboration between the Robert Steiner MRI Unit, Hammersmith Hospital (London), and the University of Sussex. TNA would like to thank Dr David Bryant for his generous scientific guidance and technical support. In addition, TNA is indebted to the Alexander Onassis Public Benefit Foundation for providing the financial support to carry out and complete this research work.

References

[1] T. W. Anderson. *The Statistical Analysis of Time Series.* Wiley, New York, 1971.

[2] T. N. Arvanitis. A model for magnetic resonance image formation. In C. Wood, R. Davidge, and P. Costa, editors, *The Fifth White House Papers, Graduate Research in Cognitive Sciences at Sussex, CSRP 251*, pages 1–3. School of Cognitive and Computing Sciences, University of Sussex, Brighton, 1992.

[3] T. N. Arvanitis. The two-dimensional Fourier Transform (2D-FT) imaging method in MRI: A computational approach. In J. K. Brook and T. N. Arvanitis, editors, *The Sixth White House Papers, Graduate Research in Cognitive Sciences at Sussex, CSRP 300*, pages 14–18. School of Cognitive and Computing Sciences, University of Sussex, Brighton, 1992.

[4] T. N. Arvanitis. *A Study of Respiratory Motion Artifacts in Magnetic Resonance Imaging and Spectroscopy.* DPhil thesis, University of Sussex, Brighton, UK, 1994.

[5] T. N. Arvanitis. Time-series analysis of MR data: Can the Lomb-Scargle periodogram be used in the future as a diagnostic tool for the identification of systematic errors in clinical MRI? In *On-line Proceedings, JMRM Internet Conference, The Future of Magnetic Resonance in Medicine*, Kyoto, Japan, 1997.

[6] T. N. Arvanitis, D. J. Bryant, A. G. Collins, G. A. Coutts, and A. S. Hall. An investigation of motion artefact in spectroscopic CSI. In *Proceedings of the 12th annual meeting of the SMRM*, page 909. Society for Magnetic Resonance in Medicine, August 1993.

[7] T. N. Arvanitis and D. Watson. Overcoming respiratory motion artifacts in MRI. In *Book of Abstracts, IEE Colloquium: Medical Imaging: Image Processing and Analysis*, pages 1–3, March 1992.

[8] T. N. Arvanitis and D. Watson. Computer modelling of the two-dimensional Fourier transform imaging method in MRI. In *Meeting Program and Abstracts, Royal Society of Medicine: Spring Meeting of the Forum on Computers in Medicine*, April 1993.

[9] T. N. Arvantis and D. Watson. Can the Lomb-Scargle periodogram identify systematic errors in MR data? *British Journal of Radiology*, 70(Suppl.):102, 1997.

[10] F. J. Beutler. Alias-free randomly timed sampling of stochastic processes. *IEEE Transactions of Information Theory*, 16:147–152, 1970.

[11] D. C. Black and J. D. Scargle. On the detection of other planetary systems by astrometric techniques. *The Astrophysical Journal*, 263:854–869, 1982.

[12] R. B. Blackman and J. W. Tuckey. *The Measurement of Power Spectra from the Point of Communications Engineering.* Dover, New York, 1958.

[13] P. Bloomfield. *Fourier Analysis of Time Series - An Introduction.* Wiley, New York, 1976.

[14] Ronald N. Bracewell. *The Fourier Transform and its Applications.* McGraw-Hill, New York, 1986.

[15] J. W. Brault and O. R. White. The analysis and restoration of astronomical data via fast Fourier transform. *Astronomy and Astrophysics*, 13:169–189, 1971.

[16] A. M. Breipohl. *Probabilistic Systems Analysis: An Introduction to Probabilistic Models, Decisions and Applications of Random Processes.* Wiley, New York, 1970.

[17] E. O. Brigham. *The Fast Fourier Transform and its Applications.* Signal Processing Series. Prentice-Hall, Engelwood Cliffs, NJ, 1988.

[18] D. C. Champeney. *Fourier Transforms and Their Physical Applications.* Academic Press, New York, 1973.

[19] C. Chatfield. *The Analysis of Time Series.* Chapman-Hall, London, fourth edition, 1989.

[20] D. G. Childers. *Modern Spectrum Analysis.* IEEE Press, New York, 1978.

[21] T. J. Deeming. Fourier analysis with unequally-spaced data. *Astrophysics and Space Science*, 361:137–158, 1975.

[22] W. Derbyshire. Standard phantoms for NMR imaging equipment. *Annali dell' Instituto Superiore di Sanita*, 19(1):163–7, 1983.

[23] D. F. Elliot and K. R. Rao. *Fast Transforms and Convolution Algorithms.* Academic Press, New York, 1982.

[24] A. L. Evans. *The Evaluation of Medical Images.* Adam Hilger Ltd., Bristol, 1991.

[25] D. J. Faulkner. Cepheid studies 1. more interaction in the beat Cepheid Utrianguli Australis. *The Astrophysics Journal*, 216:49–59, 1977.

[26] I. I. Gikhman and A. V. Skorokhod. *Introduction to the Theory of Random Processes.* Saunders, Philadelphia, 1969.

[27] Rafael C. Gonzalez and Richard E. Woods. *Digital Image Processing.* Addison-Wesley Publishing Company, Reading, Massachusetts, 1992.

[28] D. F. Gray and K. Deskachary. A new approach to periodogram analyses. *The Astrophysics Journal*, 181:523–530, 1973.

[29] D. M. Green and J. A. Swets. *Signal Detection Theory and Psychophysics.* Wiley, New York, 1966.

[30] E. J. Groth. Probability distributions related to power spectra. *The Astrophysical Journal Supplement Series*, 29(286):169–189, 1975.

[31] Joseph V. Hajnal, Ralph Myers, Angela Oatridge, Jane E. Schwieso, Ian R. Young, and Graeme M. Bydder. Artifacts due to stimulus correlated motion in functional imaging of the brain. *Magnetic Resonance in Medicine*, 31:283–291, 1994.

[32] J. C. Hancock and P. A. Wintz. *Signal Detection Theory.* McGraw-Hill, New York, 1966.

[33] J. R. Higgins. A sampling theorem for irregularly spaced sample points. *IEEE Transactions of Information Theory*, 22:621–622, 1976.

[34] J. H. Horne and S. L. Baliunas. A prescription for period analysis of unevenly sampled time series. *The Astrophysical Journal*, 302:757–763, 1986.

[35] G. M. Hyman and D. Booth. *Multivariate Time Series Analysis for Local Forecasting.* Number 11 in Occasional Papers. Centre for Environmental Studies, London, 1980.

[36] G. M. Jenkins and D. G. Watts. *Spectral Analysis and its Applications.* Holden-Day, San Francisco, 1968.

[37] .R2es

[45] A. Papoulis. *Signal Analysis*. McGraw Hill, New York, 1977.

[46] A. Papoulis. *Probability, Random Variables, and Stochastic Processed*. McGraw-Hill, New York, second edition, 1984.

[47] E. Parzen. *Stochastic Processes*. Holden-Day, San Francisco, 1962.

[48] E. Parzen. *Time Series Analysis Papers*. Holden-Day, San Francisco, 1976.

[49] W. H. Press and G. B. Rybicki. Fast algorithm for spectral analysis of unevenly sampled data. *The Astrophysical Journal*, 338:277–280, 1989.

[50] William H. Press, Saul A. Teukolsky, William T. Vetterling, and Brian P. Flannery.